Polish J. Chem., **76**, 457–470 (2002)

The Microcrystals of BEDT-TTF and BEDO-TTF Polyiodides Forming the Conducting Networks within Polymer Film Surface and Their Transformations*

by A. Tracz

Center of Molecular and Macromolecular Studies Polish Academy of Sciences, Sienkiewicza 112, 90-363 Łódź, Poland

(Received July 2nd, 2001; revised manuscript November 21st, 2001)

New results on morphology and structure of microcrystals of bis-(ethylenedithio)tetrathiafulvalene (BEDT-TTF or ET) and bis(ethylenedioxy)tetrathiafulvalene (BEDO-TTF or BO) polyiodide salts formed within surface layers of polymer films by a two step reticulate doping technique and their transformations are discussed. The architecture of the microcrystalline conducting network was studied by STM and AFM. X-ray diffraction studies of microcrystals of ET salts in polymer matrix and structure-properties relationships are discussed. The thermal transformation of microcrystals of α-ET_2I_3 in polymer matrix to β-ET_2I_3 was followed *in situ* by X-ray diffraction and a new example of the transformation of microcrystals of BO salt in polymer matrix by annealing is shown.

Key words: organic superconductors, BEDT-TTF, BEDO-TTF, AFM, X-ray diffraction, conducting polymer composites

Single crystals of bis-ethylenedithio(tetrathiafulvalene) (BEDT-TTF or ET) and bis-ethylenedioxy(tetrathiafulvalene) (BEDO-TTF or BO) polyiodide salts are insulators, conductors or even superconductors, depending on stoichiometry and on crystalline phase [1,2]. Among ET polyiodides the β-phase of $(ET)_2I_3$ exhibits the most interesting properties. Under normal pressure β-$(ET)_2I_3$ shows a superconducting transition at $T_c \approx 1.3$–1.4 K (β_L-phase). The ordering of ethylene groups in the ET molecules under moderate pressure (< 1.5 kbar) results in a transformation from the β_L to the $\beta_H(\beta^*)$-phase with $T_c \approx 8$ K [1,2]. The application of a higher pressure suppresses the transition both in the low-T_c and in the high-T_c states of β-$(ET)_2I_3$ [3,4]. Two β-like modifications of $(ET)_2I_3$ with high T_c under normal pressure were found: α_t-$(ET)_2I_3$ [5,6] (a product of thermally converted α-$(ET)_2I_3$) and β_{CO}-$(ET)_2I_3$ obtained as microcrystalline powder by chemical reaction at elevated temperature [7,8]. The most important in the BO polyiodides family is $(BO)_{2.4}I_3$ salt, which is metallic down to liquid helium temperature [9]. Tiny single crystals or microcrystalline powder of β-$(ET)_2I_3$ or $(BO)_{2.4}I_3$ are not suitable for possible applications. Therefore, polycrystalline layers obtained by evaporation of solid salts in high vacuum were studied [10–14]. Microwave absorption measurements proved that a fraction of the

*Dedicated to the memory of Professor Krzysztof Pigoń.

$(ET)_2I_3$ salt forming the layer was a bulk superconductor. However, these layers [10–13] and the layers of BO polyiodide [14] were semiconducting in d.c. conductivity measurements.

An interesting way of preparation of thin layers of organic conductors is a two-step reticulate doping technique [15]. According to it, surface conducting polymer/organic conductor composites can be obtained by the treatment of polymer (*e.g.* poly(bisphenol-A) carbonate (PC)) film containing molecularly dispersed donor (*e.g.* ET or BO) with vapors of acceptor (*e.g.* iodine) solution. Using ET and the vapors of iodine solutions, the microcrystals of α-$(ET)_2I_3$ are formed in most cases [16,17]. The microcrystals of β-$(ET)_2I_3$ can be obtained also at room temperature, but the PC films with molecularly dispersed ET must contain some amount of o-dichlorobenzene [16]. However, a more effective way of obtaining β-$(ET)_2I_3$ is the vapor treatment at higher temperatures (90–110°C), using the iodine solution in trichloroethylene or chlorobenzene [18], thus, except the presence of the polymer, the crystallization conditions resemble the conditions for obtaining β_{CO}-$(ET)_2I_3$ [7,8]. By annealing, the network of α-$(ET)_2I_3$ in PC films can be transformed to the network of α_t-$(ET)_2I_3$ and, thus, the films showing an onset of the superconducting transition at 5–6 K were obtained [19–23]. If PC films with molecularly dispersed BO are exposed to the vapors of iodine solutions, the microcrystals of conducting $(BO)_{2.4}I_3$ or of insulating $(BO)I_3$ salts are formed [24,25]. Using solutions of bromine for the vapor treatment, microcrystals of $(BO)_2Br(H_2O)_3$ can be obtained [24,25]. Solutions of other acceptors, like ICl, IBr, can also be used [26].

In this work new results expanding and verifying the knowledge on morphology, structure and transformations of crystalline ET and BO salts formed within the surface layer of polymer films are reported. The most important results concern: the thickness of the microcrystals studied by AFM on specially etched samples, analysis of the positions and relative intensities of the X-ray diffraction peaks of ET_2I_3 salts, thermal transformation of microcrystals of α-ET_2I_3 studied *in situ* by X-ray diffraction and structural transformation of the microcrystals of $(BO)I_3$ in polymer matrix to $(BO)_{2.4}I_3$ by annealing.

EXPERIMENTAL

The surface conducting polymer films were prepared by the two step reticulate doping technique [15]. In the first step, a polymer film (*e.g.* poly(bisphenol-A)carbonate (PC)) with a low amount (*e.g.* 1–2 wt.%) of molecularly dispersed donor (ET or BO) is prepared by casting from o-dichlorobenzene solution at 393 K. In the second step, the surface of such a film is exposed at room or at elevated temperature [18] to vapors of an acceptor solution (*e.g.* iodine) in a solvent able to swell the polymer. Crystallization of the salt occurs within the surface layer of the swollen polymer film. Through the following text the second step will be called "vapor treatment".

X-ray diffraction studies were performed using Siemens Diffractometer with Ni-filtered Cu-K_α radiation (λ = 1.541 Å). Annealing experiments were performed for samples closely packed in Al foil or for samples unprotected against the iodine loss. The transformation of α-$(ET)_2I_3$ to α_t-$(ET)_2I_3$ microcrystals by annealing of *PC*/α-$(ET)_2I_3$ film in the range 300–420 K was followed by *in situ* X-ray diffraction on

the unprotected samples. The diffraction experiment at given temperature was completed within 90 min. When a diffraction experiment at a certain temperature was finished, a new run of the diffractometer was started after 15 min at a temperature 10 K higher.

Morphology of samples was examined by scanning electron microscopy (SEM) using a Jeol JEM-100CX-ASID microscope in the scanning mode or by atomic force microscopy (AFM), using a Nanoscope III (Digital Instruments) as described earlier [17]. Images of the microcrystals surfaces with atomic resolution were obtained, using scanning tunneling microscopy (STM) with an apparatus made in University of Lodz. Absorption spectra were registered, using Lambda 9 UV-Vis-NIR spectrophotometer. The microcrystals of α-$(ET)_2I_3$ or $(BO)_{2.4}I_3$, forming a conducting network within the surface layer of PC films, were etched by immersing in HNO_3 for 10 sec. The etched sample was immediately washed in distilled water and dried.

RESULTS AND DISCUSSION

Microcrystals – the elements forming the conducting networks. The microcrystals of ET and BO salts, obtained by the two step reticulate doping, are small and therefore SEM, AFM or STM have to be used for morphological studies. Acceptor (*e.g*. iodine) concentration, kind of solvent, time and a temperature of vapor treatment have a strong influence on the properties of the microcrystals, including their composition *i.e*. donor-to-acceptor ratio and the crystalline phase, and also determine the formation of the conducting network and its morphology [16,17,25]. If the vapors of the solution with high iodine concentration (30–50 mg/ml) are used, the habit of the microcrystals is poorly developed [16,17]. On the contrary, when the iodine concentration is low (several mg/l), the salt crystallizes as well-formed plate-like microcrystals. It is even possible to distinguish between the microcrystals of different salts, comparing their habits with those of a single crystal. At the beginning of the vapor treatment, due to iodine deficiency within the surface layer of the swollen polymer film, the crystallization of the neutral ET, as needle-like crystals, is at the beginning of the vapor treatment also observed [16]. The microcrystals can be imaged by both AFM and STM (Figure 1). It proves that the polymer does not cover their surface. The plate-like microcrystals, seen on the film surfaces, are thin (*ca* 30 nm) (Figure 1a,b). While in the images obtained using SEM the crystals surface seems to be featureless, in the AFM images of the microcrystals surfaces different dot-like objects, various defects, some layers [17] and the molecular terraces can be seen ([16], Figure 1c,d). The difference between the interlayer spacing *d* of α-ET_2I_3 and of β-ET_2I_3 is *ca* 2 Å, thus the measurements of the height of the terraces, using AFM or STM, allow distinguishing the microcrystals of the two phases. Images with molecular resolution, similar to those obtained for single crystals [27] can be obtained (Figure 1f).

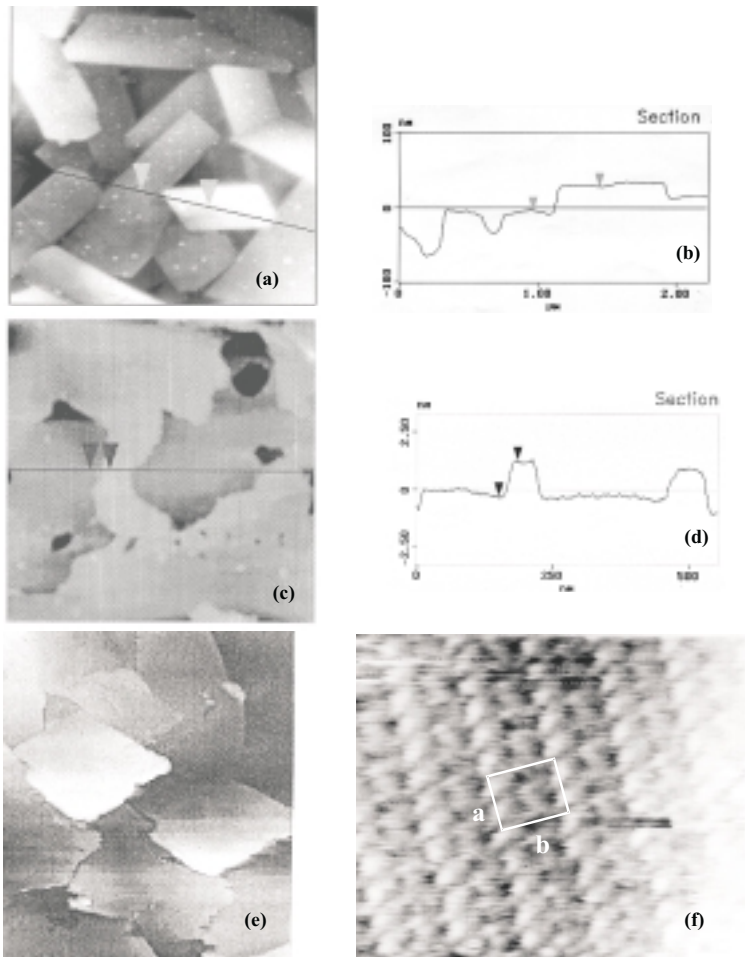

Figure 1. (a) and (b) – AFM image and its cross-section profile of the surface of PC/β-$(ET)_2I_3$; (c) and (d) – AFM image and cross-section profile of the monolayer terrace on the surface of the α-$(ET)_2I_3$ microcrystal in PC/α-$(ET)_2I_3$; (e) – STM image (2.5 × 2.8 μm) of the PC films with α-$(ET)_2I_3$ microcrystals; (f) – STM image (5.6 × 4.9 nm) of a spot on microcrystal surface shown in (e) with higher magnification. Unit cell of the cation layer is indicated.

Architecture of the conducting network. The plate-like microcrystals lie flat within the surface layer of the polymer film [16–18,25]. Some crystals are located on a higher level (more exposed), while others are situated beneath. In SEM or AFM images one can see at most three layers of microcrystals (Figure 1) [16–18,25].

The salt formation during the second step of the reticulate doping (vapor treatment) is very effective. This can be concluded from the disappearance of the absorption, related to the neutral donor molecularly dispersed in the polymer matrix (*e.g.* [17,25]). Let us assume that all donor molecules (*e.g.* ET) are consumed during the crystallization of the salt (*e.g.* $(ET)_2I_3$). Under such assumption 2 wt. % of molecularly dispersed ET gives 2.9 wt. % of the salt $(ET)_2I_3$, whose density is $\rho_s = 2.2$ g/cm^3.

Assuming that the salt forms a single crystalline plate, covering the polymer film surface, its thickness is $x = 0.029h\rho_p/\rho_s$, where h is the thickness of the film and $\rho_p \sim 1$ g/cm^3 is the density of the polymer. For the film *ca* 15 μm thick, the thickness of such crystalline plate would be *ca* 200 nm. Comparison of this estimated thickness with the thickness of microcrystals seen on the sample surface (*e.g.* 30 nm as shown in Figure 1) leads to the conclusion, that the majority of the microcrystals are embedded in the polymer matrix. This can be visualized by etching of the surface conducting films with *e.g.* HNO_3. In Figure 2 one can see the etch pits. Their shape corresponds to the shape of the microcrystals (α-$(ET)_2I_3$ or $(BO)_{2.4}I_3$). The depth of the pits (> 150 nm) is however bigger than the average thickness of the crystals seen on the surfaces. This result clearly shows that the network is not uniform across its thickness. It consists of thin microcrystals exposed on the surface (not covered by the polymer) and also of thicker ones, embedded in the polymer matrix. As it will be shown later on, the shrinkage of the polymer matrix exerts on the microcrystals a pressure and hence affects their structure and superconducting properties.

Structure. Examples of the X-ray diffraction patterns of surface conducting PC films with the microcrystals of different salts are shown in Figure 3. Due to the preferential orientation of the microcrystals, the diffractograms show only the family of (*00l*) reflexes. Comparison with the literature data is therefore limited to only one structural parameter – the interlayer spacing *d*. On the other hand, the unit cell parameters of some salts *e.g.* α-$(ET)_2I_3$ or β-$(ET)_2I_3$, determined by different groups, are slightly but significantly different. The interlayer spacing *d* calculated for different unit cell parameters of α-ET_2I_3 and of β-ET_2I_3 are compared in Table 1 and Table 2 respectively. As one can see, the differences of the interlayer spacing calculated from different unit cell parameters, amounts to *ca* 0.09 Å for α-ET_2I_3 and to *ca* 0.05 Å for β-ET_2I_3.

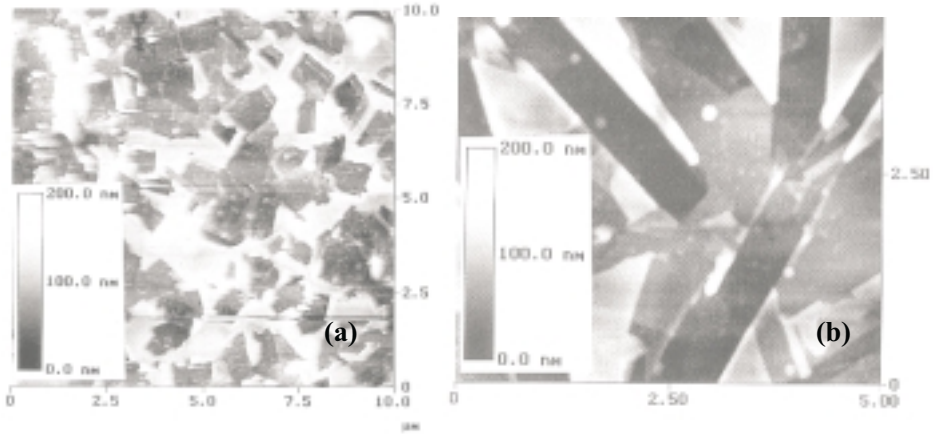

Figure 2. AFM images of the surface of PC composite films obtained by the two step reticulate doping technique after etching of the conducting microcrystals by immersing the film in HNO_3: (a) – PC/α-$(ET)_2I_3$ and (b) – PC/$(BO)_{2.4}I_3$.

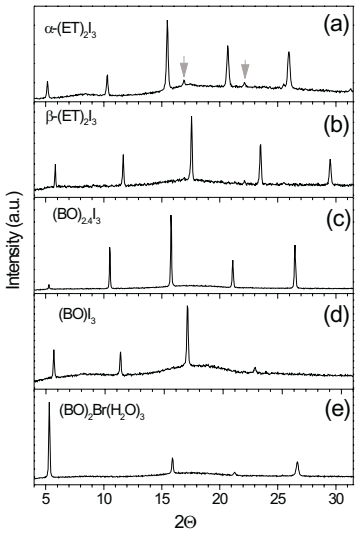

Figure 3. X-ray diffraction patterns (family of (*00l*) reflexes) of PC films with the polycrystalline networks of the microcrystals of different salts: (a) – α-$(ET)_2I_3$ [17]; (b) – β-$(ET)_2I_3$ [18], (c) – $(BO)_{2.4}I_3$ [25]; (d) – $(BO)I_3$; (e) – $(BO)_2Br(H_2O)_3$ [25]. The arrows mark the diffraction peaks related to the microcrystals of neutral ET.

Comparison of the X-ray diffraction patterns for reticulate doped films with those reported for thin layers, obtained by vacuum deposition, is also difficult. The results obtained in different laboratories for nominally the same salt are different. For instance the positions of the (*001*) diffraction peak for the layers of α-ET_2I_3 published in different papers *i.e.* 2θ = 4.98° in [10], 5.04° in [11] or 5.22° in [35] for the same X-ray wavelength 1.541 Å differs considerably. The corresponding values of *d*: 17.735 Å, 17.524 Å and 16.920 Å are different also from the values calculated from the unit cell parameters of this salt (Table 1). It does not necessarily imply that the structure of the investigated samples was really different. Small disagreement of peaks position can be due to some differences in geometrical configuration of the measurement *e.g.* the calibration of the instrument and/or in the position of the sample in the diffractometer. This is of big importance, especially if a sample is very thin. On the other hand, even the position of the diffraction peaks for different samples is similar, one should consider the relative intensities of the peaks (the shape of the diffractogram).

Table 1. The values of the interlayer spacing *d* calculated from the unit cell parameters of α-ET_2I_3 determined by different authors.

a [Å]	b [Å]	c [Å]	α [°]	β [°]	γ [°]	***d*** **[Å]**	ref.
9.172	10.785	17.390	96.96	97.92	89.13	**17.100**	[28]
9.182	10.801	17.412	96.97	97.94	90.77	**17.119**	[8]
9.183	10.804	17.442	96.96	97.93	90.85	**17.149**	[29]
9.211	10.850	17.488	96.95	97.97	90.75	**17.194**	[30]

Table 2. The values of the interlayer spacing *d* calculated from the unit cell parameters of β-ET_2I_3 determined by different authors.

a [Å]	b [Å]	c [Å]	α [°]	β [°]	γ [°]	***d*** **[Å]**	ref.
6.597	9.070	15.243	94.33	95.56	109.73	**15.155**	[31]
6.609	9.083	15.267	94.37	95.62	109.78	**15.177**	[32]
6.608	9.087	15.268	94.41	95.56	109.76	**15.179**	[8]
6.615	9.100	15.286	94.38	95.59	109.78	**15.197**	[33]
6.615	9.097	15.291	94.35	95.55	109.75	**15.204**	[34]

In Figure 4 the relative intensities of the (*00l*) diffraction peaks, calculated for the diffractograms published for polycrystalline layers of β-$(ET)_2I_3$ or α_t-$(ET)_2I_3$ and from the theoretical diffractogram for β-ET_2I_3 are compared. Different relative intensities of the diffraction peaks shown in Figure 4, unambiguously indicate on different distribution of the electron density in the direction perpendicular to the (*00l*) planes. This means, that although the average interlayer spacing in the microcrystals, forming the layers described in [10,11], is similar, their chemical composition (*e.g.* the iodine content) was slightly different. The diffractogram for the microcrystals of β-ET_2I_3 in polymer film agrees well with the theoretical one (compare Figure 3b and Figure 4d).

Taking into account the above-discussed problems, the recent studies on the microcrystals structure in reticulate doped films were performed with a great caution. It was found that the interlayer spacing *d* in the microcrystals of ET salts in reticulate doped films is slightly different than in single crystals [36]. Moreover, its value is dependent on the conditions of the film surface solidification during drying [37]. This was explained by the non-uniform stress, arising during drying when the microcrystals are forced to contact each other within and/or on the surface of the swollen polymer film [37]. When drying begins, the microcrystals "flowing" on the surface of

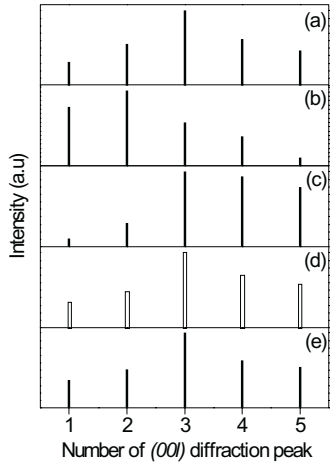

Figure 4. The relative intensities of the (*00l*) diffraction peaks calculated for: (a), (b) and (c) the diffractograms of the polycrystalline layers of β-$(ET)_2I_3$ obtained by evaporation published in [12], [10] and [13] respectively; (d) – the theoretical diffractogram for β-ET_2I_3 [38] and (e) the diffractogram of PC/β-ET_2I_3 shown in Fig. 3b.

the swollen polymer film coalesce, climb one on another and grow together, forming a polycrystalline layer (polycrystalline "skin"). Further drying results in freezing of the stress, due to the shrinkage of the viscous polymer solution. It was shown, that this stress could be relaxed by a treatment of the sample surface with the solvent vapors, able to swell the polymer or by annealing at the temperature higher than the glass transition temperature (Tg) of the polymer [37]. The difference between the interlayer spacing in microcrystals before and after relaxation can be as large as 0.1 Å. This structural change is accompanied by the changes of the optical (Raman scattering) and electrical properties [37].

The value of d ~15.09 Å, determined for β-$(ET)_2I_3$ in the relaxed polymer films is different than the values of d calculated from the unit cell parameters (Table 2). In particular, it is by *ca* 0.09 Å smaller than the value calculated from the unit cell parameters of β_{CO}-$(ET)_2I_3$ ([8], Table 2). It is, therefore, of importance to analyze the experimental diffraction data for β_{CO}-$(ET)_2I_3$ [38]. The experimental values of the 22 related to the (*001*), (*002*), (*003*), (*004*) and (*005*) diffraction peaks for the radiation wavelength 0.94468 Å are 3.588°, 7.188°, 10.776°, 14.384° and 18.008°, respectively. These values correspond to the interlayer spacing d ~15.09 Å, that is the same as determined for $(ET)_2I_3$ in the relaxed reticulate doped films [37]. The disagreement between the d values calculated from the unit cell parameters (15.18 Å) and calculated directly from the 2θ values, corresponding to (*00l*) diffraction peaks (15.09 Å), results evidently from the approximations, which have been used in calculation of the unit cell parameters.

The phenomenon, occurring during the final stage of the conductive layer solidification, leading to the coalescence of the microcrystals, is characteristic of the process of the conducting network formation in the two step reticulate doping. It results in very good contacts between the microcrystals and, hence, the electrical properties of the conducting network formed at optimum conditions are similar to those of single crystals. The temperature dependence of d.c. and a.c. conductivity of the PC films with plate-like microcrystals of α-$(ET)_2I_3$ obtained at optimum conditions show an anomaly related to the metal-insulator transition observed in a single crystal of this salts at 135 K [39]. The networks of plate like microcrystals of β-$(ET)_2I_3$ or $(BO)_{2.4}I_3$ show the metallic temperature dependence of the d.c. conductivity [24,25]. It is a big advantage of these materials over the polycrystalline layers obtained by vacuum deposition, which do not show metallic properties in the d.c. conductivity measurements [10–14].

Are the superconducting properties of the organic crystal in polymer matrix preserved? The shrinkage of the polymer matrix during cooling exerts on the microcrystals a pressure. This phenomenon has an important influence on their superconducting properties, since the temperature of the superconducting transition (Tc) for β-$(ET)_2I_3$ decreases with the applied pressure with a rate *ca* 0.75–1.2 K/kbar, depending on whether the applied pressure is hydrostatic or "non-hydrostatic" (shear component) [3,4]. The Tc ≈ 5÷6 K observed for annealed films of PC/α-$(ET)_2I_3$ was lower than expected for polycrystalline α_t-ET_2I_3 or β_H-$(ET)_2I_3$ (*ca* 8 K). This was

tentatively ascribed to the presence of structural defects [21]. It was, however, assumed that the structure of the microcrystals in polymer films at low temperature is the same as in the α_t-$(ET)_2I_3$ (or β_H-$(ET)_2I_3$) crystals without polymer. However, it was found recently, that upon cooling, the interlayer spacing *d* in β-$(ET)_2I_3$ (or α_t-$(ET)_2I_3$) in polymer composites decreases considerably stronger than in the microcrystals without polymer [40]. The effect is attributed to the pressure exerted on the microcrystals by contraction of the polymer matrix. This pressure is responsible for suppressing the superconductivity in surface conducting polymer/β-ET_2I_3 composites below 8 K. Other evidences that the shrinkage of the polymer matrix exerts on microcrystals a pressure that is high enough to change the superconducting properties of β-$(ET)_2I_3$ come from studies on mixtures of the microcrystalline powder of β_{CO}-$(ET)_2I_3$ with PC or with paraffin [41]. It was shown that the superconducting properties of these composites (the superconducting volume fraction and the temperature Tc) depend on the concentration of the β_{CO}-$(ET)_2I_3$ in the polymer matrix and on the kind of the polymer. According to recent work of H. Müller *et al.*, β_{CO}-$(ET)_2I_3$ appeared to be a mixture of the ordered phase of $\beta^*(\beta_H)$-$(ET)_2I_3$ (Tc *ca* 8 K) and disordered β_L-phase (Tc =1.4÷1.8 K) [42]. The pressure related to the shrinkage of the paraffin was moderate. However, it was sufficient to induce the transformation of $(ET)_2I_3$ from β_L- to β_H-phase. Hence, the superconducting volume fraction in β_{CO}-$(ET)_2I_3$ in paraffin composites was several times bigger than in β_{CO}-$(ET)_2I_3$ powder without polymer. The onset of the superconducting transition was observed at *ca* 8 K as expected for high Tc phase. On the contrary, the contraction of the PC matrix was large enough to suppress the superconducting transition below 8 K.

The results presented above show that the polymer is not just an "inert matrix" (although it is electrically insulating), but in some sense it is an active component of the composite during cooling. Since all organic superconductors are sensitive to pressure, the shrinkage of the polymer matrix should be taken into account, when preparing composites with polymers.

Transformation of conducting networks by annealing. Thermal induced transformation of different ET polyiodides to other phases was discovered several years ago [1], however, its mechanism was not studied. A well known example is the thermal conversion of α-$(ET)_2I_3$ to the superconducting salt α_t-$(ET)_2I_3$ (Tc *ca* 8 K, under normal pressure) [5,6]. At elevated temperature ET or BO polyiodides are not resistant against the iodine evolution. The annealing of PC/α-$(ET)_2I_3$ films in air without any protection lead to a considerable decrease of their conductivity. Moreover, the samples exhibit the semiconducting temperature dependence of the d.c. conductivity. Assuming that α_t-$(ET)_2I_3$ is stable up to 423 K, it was explained, that the evolution of iodine from α-$(ET)_2I_3$ has a higher rate than the process of α-$(ET)_2I_3$ to α_t-$(ET)_2I_3$ conversion. Consequently, the amount of the superconducting α_t-$(ET)_2I_3$ is too small to form a continuous conducting network [21]. The superconducting properties were found for the films annealed in the iodine atmosphere or for the samples that were closely packed in a Al foil.

In-situ X-ray diffraction studies on the transformation process of the unprotected sample proved that a deterioration of α_t-$(ET)_2I_3$ microcrystals occurs already below 410 K. The diffractograms of PC/α-$(ET)_2I_3$ after consecutive stages of annealing are shown in Figure 5. As one can see, the intensity of the peaks related to α-$(ET)_2I_3$ decreases with increasing temperature of annealing and simultaneously the peaks corresponding to the crystalline neutral ET are growing (diffraction patterns at 300–380 K in Fig. 5). This process can be attributed to iodine escape from α-$(ET)_2I_3$ and conversion from α-$(ET)_2I_3$ to neutral ET. The transformation from α-$(ET)_2I_3$ to α_t-$(ET)_2I_3$ occurred during the time (several minutes), when the temperature of the sample increased from 390 K to 400 K. The decrease of the peaks intensity, corresponding to α_t-$(ET)_2I_3$, is clearly seen after subsequent annealing at higher temperature. This result shows that the samples should be protected against the iodine evolution not only from α-$(ET)_2I_3$ but also from α_t-$(ET)_2I_3$. The thermal conversion of α-ET_2I_3 to α_t-ET_2I_3 in PC films can also be followed by UV-Vis absorption measurements [43], Raman spectroscopy [44] or electron spin resonance [45].

For connectivity of the conducting network it is of importance whether or not the shape of the microcrystals (*i.e.* the elements forming the conducting network) is preserved after the transformation. Optical studies on the slow transformation of a thin crystal of α-ET_2I_3 suggested that the transformation proceeds *via* gradual growth of the domain of a new phase (α_t) within the body of α-ET_2I_3 and the initial shape of the crystal remains unchanged [46]. On the other hand, the statement in [6] (p. 490): "α-phase crystals tempered at 75°C kept their shapes much better than those tempered at higher temperatures." indicates that some change of the crystal habit during the transformation occurs. It was also mentioned that after the annealing the crystal

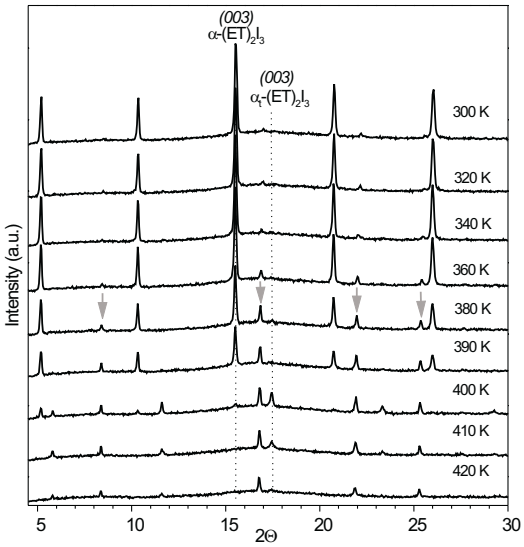

Figure 5. X-ray diffraction patterns of PC/α-$(ET)_2I_3$ at different temperatures. The most intense (*003*) diffraction peaks of α-ET_2I_3 and α_t-ET_2I_3 are indicated by dotted line. The arrows mark the diffraction peaks related to neutral ET.

surface was corrupted, due to the iodine loss [12]. No further information, however, was given.

The *ex-situ* SEM [22] and AFM studies on PC/α-ET_2I_3 have shown that the α-$(ET)_2I_3$ to α_t-$(ET)_2I_3$ transformation in reticulate doped films proceeds *via* re-crystallization (Figure 6). It means that there is no direct correlation between the morphology of α-ET_2I_3 and of α_t-$(ET)_2I_3$.

In the case of the transformation of α-$(ET)_2I_3$ to α_t-$(ET)_2I_3$ the stoichiometry of the salt is preserved. Therefore, during annealing the samples have to be protected against the iodine loss. The iodine evolution from the microcrystals is desirable in the case of the transformation of the insulating films PC/$(BO)I_3$ to the conducting films PC/$(BO)_{2.4}I_3$. The iodine content has to be decreased *ca* 4 times, therefore, the films were annealed in air without any protection. In Figure 7a the changes in the optical absorption and in the structure are shown. After annealing, the absorption band (at 1050 and 1450 nm) related to the dimers of fully-ionized (BO^+) vanishes, while the CT band responsible for the high electrical conductivity related to the charge transfer between partially charged BO molecules appears. As can see in Figure 7b, the (*00l*) reflexes corresponding to $(BO)I_3$ are after annealing changed to the reflexes of $(BO)_{2.4}I_3$.

Transformation of the conducting networks by anion exchange. The long axes of ET or BO molecules are oriented approximately normal to the film due to the preferential orientation of the microcrystals with their *ab* plane parallel to the film surface. Such orientation suppresses the intermolecular excitations induced by the perpendicular incident visible light hence donor molecules do not contribute much to

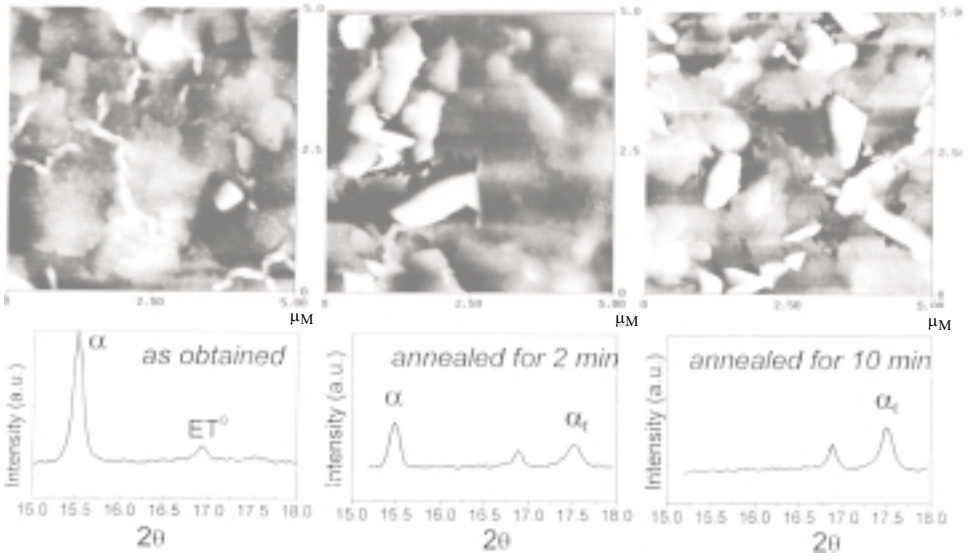

Figure 6. AFM images and X-ray diffraction of PC/α-$(ET)_2I_3$ film: as obtained (left), after annealing at 150°C for 2 min (middle) and for 10 min (right).

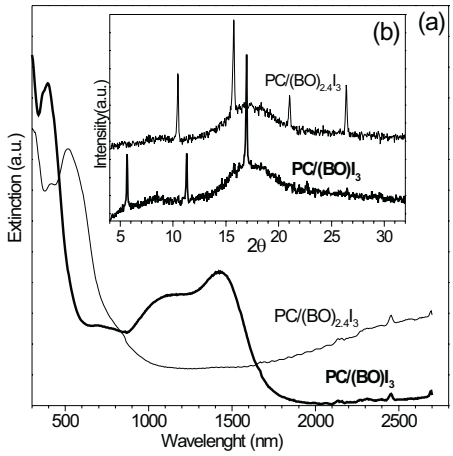

Figure 7. (a) – Absorption spectra and (b) – X-ray diffraction patterns of the, as obtained, PC/(BO)I_3 film (thick line) and after its transformation to PC/$(BO)_{2.4}I_3$ by annealing at 120°C.

the absorption. Thus, the color and the transparency of the films are dependent on the optical properties of the acceptor. Due to the strong absorption of $(I_3)^-$ anion, films with microcrystals of polyiodides of ET or BO are strongly colored [24,25]. Replacing $(I_3)^-$ anion by less absorbing or "colorless" anions *e.g.* $(IBr_2)^-$, $[I(H_2O)_x]^-$ or $[Br(H_2O)_3]^-$ is a new way of obtaining transparent, colorless surface conducting polymer films [47–49]. The anion exchange may occur either *via* recrystallization or *via* intercalation. The exposure to the Br_2 vapors transforms the PC/α-ET_2I_3 (or PC/β-ET_2I_3) films into the PC/α-ET_2IBr_2 [47]. In this case the anion exchange occurs *via* recrystallization, but in spite of the reaction, which leads to a specific deterioration of the microcrystals, the continuity of the conducting is preserved. More interesting is the anion exchange *via* intercalation, since the shape of the microcrystals is preserved. Particularly the salt $(BO)_{2.4}I_3$ can be transformed to $(BO)_2I(H_2O)_x$ or $(BO)_2Br(H_2O)_3$ [49]. This can be achieved by immersing strongly colored PC/$(BO)_{2.4}I_3$ films in KBr solution or by contacting them with a Cu plate in KI solution. Colorless films, showing a metallic conductivity or semiconducting behavior, can be obtained. The $(BO)_2Br(H_2O)_x$ and $(BO)_2I(H_2O)_x$ microcrystals can reversibly change their water content, as was shown by comparative X-ray diffraction and electrical studies performed under a reduced pressure or in a dry atmosphere and under ambient conditions [49]. The colorless films derived from PC/$(BO)_{2.4}I_3$, combining two important properties: metallic conductivity and high transparency are unique among organic conducting materials or composites. Materials possessing the above properties can be considered for replacing the commonly used ITO electrodes in designing flexible, fully organic, opto-electronic systems for some specific applications.

REFERENCES

1. Williams J.M., Ferraro J.R., Thorn R.J., Carlson K.D., Geiser U., Wang H.H., Kini A.M. and Whangbo M.H., Organic Superconductors (Including Fullerenes). Synthesis, Structure, Properties and Theory, Prentice Hall, Engelwood Cliffs, NJ, 1992.
2. Ishiguro T., Yamaji K. and Saito G., Organic Superconductors (2nd Ed.), Springer-Verlag Heidelberg, 1998.
3. Schriber J.E., Azevedo L.J., Kwak J.F., Venturini E.L., Lueng P.C., Beno M.A., Wang H.H. and Williams J.M., *Phys. Rev. B*, **33**, 1987 (1986).
4. Tokumoto M., Murata K., Kinoshita N., Yamaji K., Anzai H., Tanaka Y., Hayakawa Y., Nagasaka K. and Sugawara Y., *Mol. Cryst. Liq. Cryst*., **182**, 295 (1990).
5. Baram G.O., Buravov L.I., Degtyarev L.S., Kozlov M.E., Laukhin V.N., Laukhina E.E., Onishchenko V.G., Pokhodnya K.I., Sheinkman M.K., Shibaeva R.P. and Yagubskii E.B., *JETP Lett*., **44**, 376 (1986).
6. Schweitzer D., Bele P., Brunner H., Gogu E., Haerleben U., Hennig I., Klutz I., Swietlik R. and Keller H.J., *Z. Phys. B. – Cond. Matter.*, **67**, 489 (1987).
7. Müller H., Svenson S.O., Fitch A.N., Lorenzen M. and Xenikos D.G., *Adv. Mater.*, **9**, 896 (1997).
8. Madsen D., Burghammer M., Fiedler S. and Müller H., *Acta. Cryst*., **B55**, 601 (1999).
9. Wudl F., Yamochi H., Suzuki T., Isotalo H., Fite C., Kasamai H., Liou K. and Srdanov G., *J. Am. Chem. Soc*., **112**, 2461 (1990).
10. Kawabata K., Tanaka K. and Mizutani M., *Solid State. Comm*., **74**, 83 (1990).
11. Kawabata K., Tanaka K. and Mizutani M., *Synth. Met*., **41**, 2097 (1991).
12. Moldenhauer J., Wachtel H., Schweitzer D., Gompf B., Eisenmenger W., Bele P., Brunner H. and Keller H.J., *Synth. Met*., **70**, 791 (1995).
13. Niebling U., Stein J., Schweitzer D. and Strunz W., *Solid State Comm*., **106**, 505 (1998).
14. Niebling U., Moldenhauer J., Ludwig T., Schweitzer D. and Strunz W., *Solid State Comm*., **97**, 837 (1996).
15. Jeszka J.K. and Tracz A., *Polym. Adv. Technol*., **3**, 139 (1992); Jeszka J.K., this issue, *Polish J. Chem*., **76**, 201 (2002).
16. Tracz A., Jeszka J.K., Sroczyńska A., Ulański J. and Pakula T., *Adv. Mat. Opt. Electr.*, **6**, 335 (1996).
17. Tracz A., Jeszka J.K., Pakula T. and Rabe J.P., *Synth. Met*., **94**, 17 (1998).
18. Jeszka J.K., Tracz A., Sroczyńska A., Ulański J., Müller H., Pakula T. and Kryszewski M., *Synth. Met*., **103**, 1820 (1999).
19. Müller H., Svenson S.O., Fitch A.N., Lorenzen M. and Xenikos D.G., *Adv. Mater.*, **9**, 896 (1997).
20. Ulański J., Jeszka J.K., Tracz A., Głowacki I., Kryszewski M. and Laukhina E., *Synth. Met*., **55**, 109 (1993).
21. Laukhina E.E., Merzhanov V.A., Pesotskii S.I., Khomenko A.G., Yagubskii E.B., Ulański J., Kryszewski M. and Jeszka J.K., *Synth. Met*., **69**, 797 (1995).
22. Ulański J., Tracz A., Jeszka J.K., Laukhina E., Helberg H.W. and Pakula T., *Synth. Met*., **85**, 1591 (1997).
23. Ulański J., Tracz A., Jeszka J.K., Laukhina E., Khomenko A., Polanowski P., Staerk D. and Helberg H.W., in: R.W. Munn, A. Miniewicz and B. Kuchta (Eds), Electrical and Related Properties of Organic Solid State, Kluwer Academic Pub., Dordrecht 1997, p. 241.
24. Horiuchi S., Yamochi H., Saito G., Jeszka J.K., Tracz A., Sroczyńska A. and Ulański J., *Mol. Cryst. Liq. Cryst*., **296**, 365 (1997).
25. Jeszka J.K., Tracz A., Sroczyńska A., Kryszewski M., Yamochi H., Horiuchi S., Saito G. and Ulański J., *Synth. Met*., **106**, 75 (1999).
26. Laukhina E., Tkacheva V., Shibaeva R., Khasanov S., Rovira C., Veciana J., Vidal-Gancedo J., Tracz A., Jeszka J.K., Sroczyńska A., Wojciechowski R., Ulański J. and Laukhin V., *Synth. Met*., **102**, 1785 (1999).
27. Magonov S.V., Bar G., Keller E., Yagubskii E.B., Laukhina E.E. and Cantow H.-J., *Ultramicroscopy*, **42–44**, 1009 (1992).
28. Shibaeva R.P., Kaminskii V.F. and Yagubski E.B., *Mol. Cryst. Liq. Cryst*., **119**, 361 (1984).
29. Emege J.T., Heung P.C.W., Beno M.A., Wang H.H., Williams J.M., Whangbo M.H. and Evain M., *Mol. Cryst. Liq. Cryst*., **138**, 393 (1986).
30. Bender K., Henning I., Schweitzer D., Dietz K., Endres H. and Keller H.J., *Mol. Cryst. Liq. Cryst*., **108**, 359 (1984).

31. Mori T., Kobayashi A., Sasaki Y., Kobayashi H., Saito G. and Inokuchi H., *Chem. Lett*., 957 (1984).
32. Shibaeva R.P., Kaminskii V.F. and Belskii V.K., *Sov. Phys. Crystallogr.*, **29**, 638 (1984).
33. Schultz A.J., Wang H.H. and Williams J.M., *J. Am. Chem. Soc*., **108**, 7853 (1986).
34. Bender K., Henning I., Schweitzer D., Dietz K., Endres H. and Keller H.J., *Mol. Cryst. Liq. Cryst*., **108**, 359 (1984).
35. Söderholm S., Loppinet B. and Schweitzer D., *Synth. Met*., **62**, 187(1994).
36. Tracz A., Jeszka J.K. and Pakula T., *Synth. Met*., **103**, 1972 (1999).
37. Tracz A., *Synth. Met*., **109**, 267 (2000).
38. Cambridge Crystallographic Centre, CCD-AM-C1030.
39. Polanowski P.,Tracz A., Ulański J. and Dormann E., *Synth. Met*., **109**, 235 (2000).
40. Tracz A., *Synth. Met*., **123**, 477 (2001).
41. Tracz A., Wosnitza J., Barakat S., Hagel J. and Müller H., *Synth. Met*., **120**, 849 (2001).
42. Müller H., Madsen D., Fitch A.N., Wanka S. and Wosnitza J., *J. Phys. IV*, **10**, 147 (2000).
43. Helberg H.W., Staerk D., Ulański J. and Jeszka J.K., *Acta Phys. Polon*., **87**, 893 (1995).
44. Wojciechowski R., Ulański J., Polanowski P., Lefrant S. and Faulques E., *Synth. Met*., **109**, 301 (2000).
45. Laukhina E., Ulański J., Khomenko A., Pesotskii S., Tkachev V., Atovmyan L., Yagubskii E., Rovira C., Veciana J., Vidal-Gancedo J. and Laukhin V., *J. Phys. I France*, **7**, 1665 (1997).
46. Helberg H.W., Schweitzer D. and Keller H.J., *Synth. Met*., **27**, A347 (1988).
47. Tracz A., *Synth. Met*., **109**, 273 (2000).
48. Tracz A., Jeszka J.K., Sroczyńska A., Ulański J., Horiuchi S., Yamochi H and Saito G., *Synth. Met*., **86**, 2173 (1997).
49. Tracz A., *J. Appl. Polym Sci*., in press.